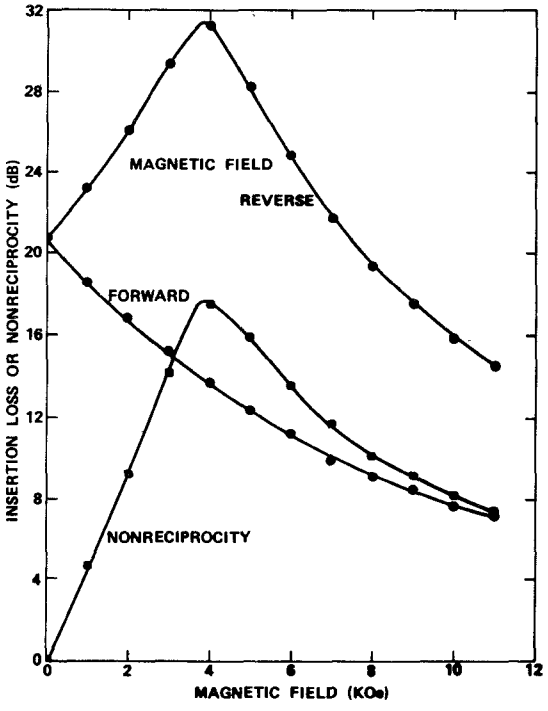

Fig. 3. Plot of insertion loss and nonreciprocity versus applied magnetic field for film 878 in the Faraday-rotation configuration with standard-size circular waveguide. The nonreciprocity curve is the difference between the forward and reverse insertion-loss curves. Film parameters: $d = 2\ \mu m$, $\mu = 5.3 \times 10^4\ cm^2/V \cdot s$, and $n = 1.2 \times 10^{16}\ cm^{-3}$.

sibly a better substrate for millimeter-wave transmission would be quartz. Unfortunately, however, quartz is not compatible with the recrystallization growth technique, because its thermal expansion coefficient is considerably different than the coefficient for InSb, and the InSb films tend to peel away from the quartz substrate.

FARADAY-ROTATION MODE

The Faraday-rotation mode configuration is shown in Fig. 1(b), and results for the Faraday-rotation mode are shown in Fig. 3. As is evident, large values of nonreciprocity are easily obtainable at relatively low magnetic fields. Very disappointing, however, are the relatively large values of insertion loss encountered, albeit they are significantly lower than the values of insertion loss for the field-displacement mode. The peak in transmission is expected and corresponds to the magnetic-field value at which the Faraday rotation in the InSb film is approximately equal to 45°. It is near this magnetic-field value that the nonreciprocity is a maximum and would be the operating point of a practical isolater. The theory of Faraday rotation in thin films, which is discussed in [4]–[7], accounts for the large values of rotation by considering multiple reflections within the film. The results in Fig. 3 were obtained on samples in standard size TE_{11} commercial waveguide (diameter is 3.58 mm). Measurements taken on samples in oversized guide (diameter is 7.1 mm) did not produce significantly different results. Essentially, the only method available to decrease the insertion loss is to make the film thinner. However, as the films are made thinner, the mobilities decrease and the extrinsic carrier concentration increases. The thickness of the films for which data are shown in Fig. 3 is 2.1 μm and is essentially as thin as the films can be grown and still have acceptable mobilities and carrier concentrations. The insertion loss due to a bare substrate in the Faraday-rotation mode is about 2 dB. A small decrease in insertion loss could be realized by using a less lossy substrate material.

CONCLUSIONS

Large values of nonreciprocity were measured for the InSb films in the Faraday-rotation mode, and these large values were obtainable at reasonably low values of the applied magnetic field. An insertion loss of 9 dB was measured, which includes 2 dB of attenuation due to the substrate, at a nonreciprocity of 10 dB. Commercially available ferrite isolators in this frequency range have insertion losses of 1.0 dB. Possibly, with a less lossy substrate material and with a high-mobility film which is 1 μm or less thick, this figure could be approached. Insertion loss with the field-displacement mode was disappointingly large and all attempts to decrease it failed.

ACKNOWLEDGMENT

The authors wish to thank H. Wieder and A. Clawson of the Naval Electronics Laboratory Center, San Diego, Calif., for furnishing the films used in this work.

REFERENCES

[1] R. J. Dinger and D. J. White, "The use of a thin vacuum-deposited InSb film as a *K*-band field displacement isolator," *Proc. IEEE* (Lett.), vol. 60, pp. 646–647, May 1972.
[2] K. Suzuki and R. Hirota, "Nonreciprocal millimeter-wave devices using a solid-state plasma at room temperature," *IEEE Trans. Electron Devices*, vol. ED-18, pp. 408–411, July 1971.
[3] A. R. Clawson, "Bulk-like InSb films by hot-wire zone crystallization," *Thin Solid Films*, vol. 12, pp. 291–294, 1972.
[4] B. Donovan and T. Metcalf, "The inclusion of multiple reflections on the theory of the Faraday effect in semiconductors," *Brit. J. Appl. Phys.*, vol. 15, pp. 1139–1151, 1964.
[5] D. J. White, R. J. Dinger, and H. H. Wieder, "Free-carrier Faraday rotation of dendritic InSb films in the microwave *X*-band region," *J. Appl. Phys.*, vol. 38, pp. 3171–3177, July 1967.
[6] D. J. White, "Room-temperature Faraday rotation in n-type InSb films at 23.4 GHz," *J. Appl. Phys.*, vol. 39, pp. 5083–5086, Oct. 1968.
[7] R. F. Dinger and D. J. White, "Possibility of using thin InSb films for Faraday rotation millimeter-wave isolators," Naval Weapons Center Tech. Publ., NWC TP 4985, Dec. 1970.

Moment Method of Calculating Discontinuity Inductance of Microstrip Right-Angled Bends

A. GOPINATH, MEMBER, IEEE, AND B. EASTER

***Abstract*—A method of estimating quasi-static discontinuity inductances in microstrip lines is outlined. Numerical results for symmetric right-angle bends are presented and compare well with experimental results.**

I. INTRODUCTION

The study of microstrip discontinuities has resulted in several papers [1]–[4] which evaluate the capacitive components of the discontinuity equivalent circuits, under static conditions. Estimating the inductive components of these equivalent circuits has received little attention to the present time. One method based on charge estimates [5], [6] is not rigorous and the results and trends published are not in agreement with experimental measurements obtained by the method of a previous publication [7]. A second method is the evaluation of these inductances based on a skin-effect formulation [8], but several difficulties have been encountered in extending this method to the accurate evaluation of discontinuity inductances. These have currently been resolved, and results are to be published shortly [9]. The present short paper outlines an alternative method based on an extension of the moment method, using current loops as elements. The method also incorporates the excess current (charge) technique used by Benedek and Silvester [10] for preserving the accuracy of calculated parameters. This short paper outlines the formulation used and presents specific results for symmetric right-angled bends. It is hoped a subsequent paper will present a comprehensive set of results of various other discontinuities.

II. STATEMENT OF PROBLEM

The moment method of inductance estimation outlined here can be used for a variety of strip geometries, but is illustrated only for the case of the symmetrical right-angle bend. We first define in the

Manuscript received January 1, 1974; revised May 14, 1974.
The authors are with the School of Electronic Engineering Science, University College of North Wales, Bangor, Caerns., Wales.

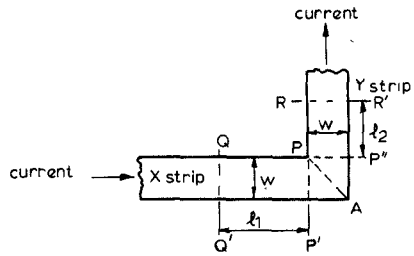

Fig. 1. Plan view of symmetric microstrip bend showing reference planes PP', PP'' and QQ', RR'. Strip width is w, ground plane spacing h.

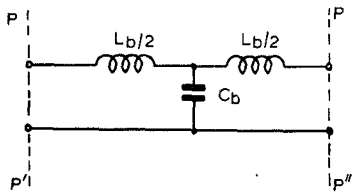

Fig. 2. Equivalent circuit of the symmetric right-angled bend in microstrip, at the references planes PP' and PP'' as defined in Fig. 1.

context of this bend the equivalent-circuit components that require evaluation. In Fig. 1, the plan view of the microstrip bend is shown. The bend occurs at the junction of two semi-infinite strips (X and Y strips in Fig. 1). It is convenient to define the inductance of the bend with respect to the reference planes PP' and PP''. However, the fringing fields associated with the bend will extend a significant distance beyond these reference planes. In order to calculate the inductance it is necessary to introduce the reference planes QQ',RR' at distances l_1,l_2 from PP' and PP'', respectively, where the current and field distributions differ negligibly from the infinite-strip distribution. The bend inductance L_b with respect to PP',PP'' can then be determined from the total magnetic field energy between QQ',RR' less an appropriate deduction for the lengths l_1,l_2:

$$L_b = L_{QR} - (l_1 L_\infty + l_2 L_\infty) \qquad (1)$$

where L_∞ is the inductance per meter of the infinite uniform strip.

The total bend capacitance C_b is similarly defined, and from the symmetry of the structure, the equivalent circuit of the bend discontinuity is usually given as in Fig. 2 by a T network. With this definition for L_b, it is possible for its numerical value to become negative.

Benedek and Silvester [10] replace the series inductances in Fig. 2 by equivalent line lengths, which however, are not given. Associated with these line lengths are capacitances which must be subtracted from C_b, which then changes the value of the shunt capacitance of their equivalent circuit. Their calculations, however, only provide C_b and not this modified capacitance, and therefore are valid only in the circuit given in Fig. 2.

III. FORMULATION OF PROBLEM AND METHOD OF SOLUTION

It will be assumed that the substrate of the microstrip line is nonmagnetic, so that the presence of the substrate may be ignored for the purpose of calculating the quasi-static inductance.

In order to obtain values which are relevant to high frequency applications, it will be further assumed that the conducting strips and ground plane have near-perfect conductivity, so that skin effect is fully established. It follows that the currents in the structure may be considered to be surface currents, infinitely thin, having zero divergence, and distributed such that the magnetic field normal to the conductor surface is zero.

For the two-dimensional problem of straight uniform microstrip, the correct distribution and inductance may be determined from the charge and capacitance of a related electrostatic problem [11], [12]. In the three-dimensional case of a discontinuity structure this procedure is not available and it is necessary to work directly in terms of the current distribution which is determined by means of a governing equation corresponding to the condition outlined above. The magnetic field energy of the structure is then computed.

If the reference planes QQ',RR' are chosen so as to include a satisfactorily large proportion of the fringing field of the discontinuity, then (1) will involve the relatively small difference of two nearly equal numbers. However, the resulting loss of accuracy may be reduced by a method analogous to that suggested by Benedek and Silvester [10].

The procedure for calculating the inductance may be formulated in the following manner.

1) Set up an assumed current distribution through the discontinuity which maintains detailed current continuity and results in the infinite-strip distribution being preserved at least until the junction reference planes PP' and PP''.

2) Set up a network of circulating currents unknown in magnitude which will effectively redistribute the previously mentioned assumed distribution.

3) Evaluate the magnitudes of the circulating currents such that the governing equation is satisfied by the current distribution obtained from the superposition of the assumed and circulating currents.

4) Evaluate the required inductances from the now known current distribution.

The moment method of implementation of this formulation results in the semi-infinite strips (see Fig. 3) being divided into substrips. The current is assumed to be constant in each of these substrips, their magnitudes are those obtained for the infinite-strip distribution, estimated by the method images [12]. Continuity of current in the symmetrical bend is preserved as shown in Fig. 3(a), where the substrips meet along the bend diagonal PA and the incoming x-directed current in each substrip of X strip flows as the outgoing y-directed current in the corresponding substrip of the Y strip. If the two X and Y strips are not of equal width, the detailed continuity is preserved by current flow along the diagonal. For the present, we only consider the symmetrical bend case where this flow is absent.

The circulating currents, in the moment method take the form of rectangular current loops which are contiguous, as shown in Fig. 3(b) for the bend. These currents redistribute the assumed current distribution of Fig. 3(a) to satisfy the governing equation. While the skin-effect equation [9] could be used here, a simpler method is to require the B_{normal} penetrating into the strip to zero. This is obtained by estimating B_{normal} (or H_z) at the center of each loop

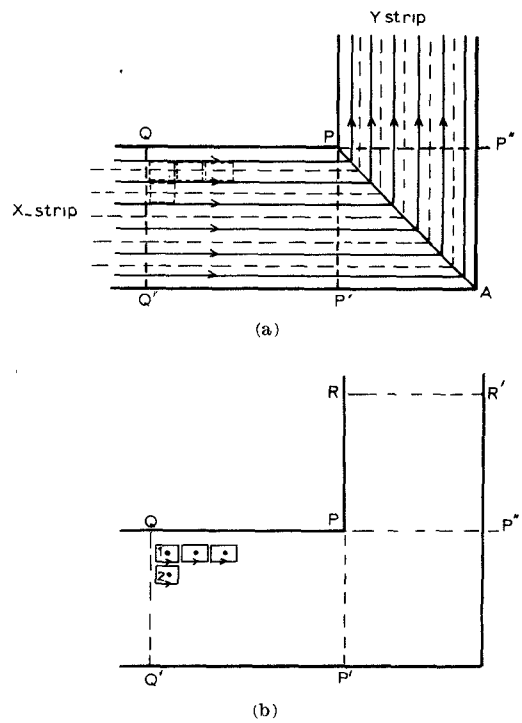

Fig. 3. (a) Discretization of infinite-strip current into substrips, with detailed continuity preserved at bend diagonal. The substrip currents are assumed constant. (b) Discretization of circulating currents into contiguous loops. Superposition of these as shown in (a) results in current redistribution.

current, due to itself, all the other unknown loop currents, and the known substrip currents, and setting this to zero. The resultant matrix equation is inverted to give the magnitude of the loop currents. Thus

$$B_z^n = 0 = \sum_{i=1}^{M} I_i^l G_l^B(r_i/r_n) + \sum_{j=1}^{i=N} I_i^{ss} G_s^B(r_j/r_n) \tag{2}$$

where

B_z^n	B_{normal} at the center of the nth loop;
I_i^l	unknown value of the ith loop current;
r_i, r_n	position of the centers of the ith and nth loops;
r_j	termination point of semi-infinite line;
$G_l^B(r_i/r_n)$	Green's function for B_z at nth loop center due to the ith loop (see Appendix I);
M	total number of loops;
I_i^{ss}	known value of the ith substrip current;
$G_s^B(r_j/r_n)$	Green's function of B_z at the nth loop center due to a semi-infinite substrip ending at r_j, over an infinite ground plane (see Appendix II);
N	number of substrips in both X and Y strips.

This leads to a matrix equation of the form

$$PI^l = f \tag{3}$$

from which I^l, the loop currents are evaluated.

To calculate the inductance, note that

$$\int \bar{A} \cdot \bar{J}\, dV = LI_t^2. \tag{4}$$

The stored energy given by this equation is calculated at each side of each loop, and summed to give the total stored energy. The current density $\bar{J}$ at each side of each loop is the net current density, due to the loop current, its adjacent contiguous loop current, and the substrip current (if either or both are present). The vector potential $\bar{A}$ is due to all the other loops, substrips, and the opposite side of the loop, and also due to the self-potential. The current I_t is the total current flowing into or out of the corner.

The contiguous current loops extend from QQ' to RR' [see Fig. 3(b)], and from (1), the subtraction of the infinite-strip inductance needs to be carried out in the inductance estimates for the rectangular regions QQ' to PP' and PP'' to RR'. For these regions (1) and (4) become

$$L_e = L_{\text{tot}} - (l_1 + l_2)L_\infty = \frac{1}{I_t^2}\left| \int \bar{A}_t \bar{J}_t\, dV - \int \bar{A}_\infty \cdot \bar{J}_\infty\, dV \right|. \tag{5}$$

Now let

$$\bar{A}_t = \bar{A}_e + \bar{A}_\infty$$

where $\bar{A}_e$ is the excess potential and

$$\bar{J}_t = \bar{J}_e + \bar{J}_\infty$$

where $\bar{J}_e$ is the excess current. Thus

$$L_e = \frac{1}{I_t^2} \int_v (\bar{A}_e \cdot \bar{J}_\infty + \bar{A}_\infty \cdot \bar{J}_e + \bar{A}_e \cdot \bar{J}_e)\, dV. \tag{6}$$

For the rectangular region $PP''PP'$, the whole of the inductance as given by (4) is estimated, and the sum of these inductances is equal to the required value L_b.

We note that the vector potential $\bar{A}$ due to a filamentary current at any point on itself results in a singularity which cannot be evaluated. Thus it becomes necessary to assume that the loop current is distributed evenly over each side, now assumed to be a strip as shown in Fig. 5 and the mean position of which is the rectangular loop filament. A similar scheme is necessary to estimate the vector potential of the semi-infinite substrip on itself. The result of this scheme for the loop currents is that the inductance is calculated with each side of each loop current assumed to be distributed in strip form and therefore each loop is assumed to start (and end) at the edge of this strip. Thus the reference planes for the discontinuity and the associated circulating currents are unambiguously defined.

The necessary functions for estimating $\bar{A}$ in equations (4) and (6) are given in the Appendices. The volume integrals in these equations become line integrals when the net current due to the loop, its adjacent contiguous loop current and substrip currents (if either or both are present) are assumed to be uniform over the width of loop (strip) side.

Thus

$$\int_v \bar{A} \cdot \bar{J}_{\text{net}}\, dV = \int \bar{A} \cdot \bar{I}_{\text{net}}\, dl \simeq 2l_i(\bar{A} \cdot \bar{I}_{\text{net}}) \tag{7}$$

where $2l_i$ is the loop side length. However, when this integral is evaluated over the side due to its own vector potential, this is modified as shown in (A.3) (see Appendix I).

IV. RESULTS AND DISCUSSION

A computer program was developed for estimating the discontinuity inductance of symmetric right-angle bends. The parameters that form the input data are the w/h ratio, and the coordinates of the rectangles shown in Fig. 1. The number of substrips and current loops are also variables. As the substrip number N increases, the number of current loops M increases as some function of the square of N. Thus runs were carried out for N varying from 3 to 6, and the corresponding M varying from 16 to 85, for unit distance boundaries (QQ' and RR') from the reference planes (PP' and PP'', respectively). The boundary distances may be increased at the expense of substrip number, and some further calculations were also performed with these for comparison with N varying up to 5 and M with a maximum of 120. The infinite-strip inductances L_∞ for the various w/h for N varying from 3 to 6 were in error from about 4 percent to less than 2 percent. The results obtained are summarized in Fig. 4 after extrapolation, and are expected to be accurate to within a few percent (expressed in terms of width of strip as unity), mainly due to the poor discretization.

Also shown in Fig. 4 are experimental results obtained by the method reported elsewhere [7]. These data were obtained by comparing the resonant conditions of symmetrical "L" shaped resonators of $\lambda/2$ or $3\lambda/2$ effective overall length with corresponding linear

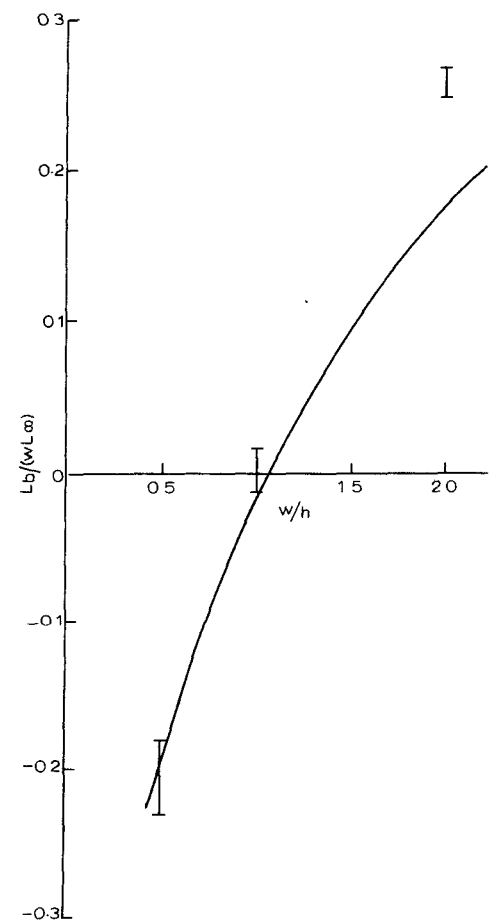

Fig. 4. Variation of normalized inductance of microstrip corner L_b with w/h ratio. Normalization is over wL_∞. ---: theory; I: experimental bars.

resonators. Since for these modes of resonance there is a voltage node at the corner, the effect of the corner capacitance C_b may be ignored and the corner inductance L_b can be determined from the difference in effective length of the two types of resonator. The end effects at the open ends including the effect of the input coupling, and the microstrip velocity were determined by an initial measurement involving linear resonators of different lengths. The measurements were performed on 0.660-mm alumina in the frequency range 4–10 GHz, and the results extrapolated to zero frequency. The accuracy of measurement, expressed as a line length, is estimated as ± 10 μm.

The experimental and predicted values agree closely for values of $w/L \leq 1.5$, but diverge for larger w/L. The effect of the crude discretization of the theoretical model worsens as the width of the strip and hence that of each substrip becomes comparable to the ground plane spacing, leading to errors in the predicted values.

A clear limitation of this method is that the quasi-static formulation cannot predict frequency variation of the inductance values. However, the experimental work outlined above indicates that the quasi-static parameters have a useful range of approximate validity. It is hoped to report on these aspects of measurements in greater detail in a later publication.

APPENDIX I
GREEN'S FUNCTIONS FOR CURRENT LOOP

Field strength H_z at $P(x_1,y_1,z_1)$ due to current loop unit current in the $z = 0$ plane is calculated:

H_z^x (due to x-directed currents)

$$= \frac{1}{4\pi}\left\{\left[\frac{(x_1 - l_1)(y_1 - l_2)}{\{(y_1 - l_2)^2 + z_1^2\}r_1} - \frac{(x_1 + l_1)(y_1 - l_2)}{\{(y_1 - l_2)^2 + z_1^2\}r_2}\right]\right.$$

$$\left. - \left[\frac{(x_1 - l_1)(y_1 + l_2)}{\{(y_1 + l_2)^2 + z_1^2\}r_3} - \frac{(x_1 + l_1)(y_1 + l_2)}{\{(y_1 + l_2)^2 + z_1^2\}r_4}\right]\right\}$$

H_z^y (due to y-directed currents)

$$= \frac{1}{4\pi}\left\{\left[\frac{(x_1 - l_1)(y_1 - l_2)}{\{(x_1 - l_1)^2 + z_1^2\}r_1} - \frac{(x_1 - l_1)(y_1 + l_2)}{\{(x_1 + l_1)^2 + z_1^2\}r_3}\right]\right.$$

$$\left. - \left[\frac{(x_1 + l_1)(y_1 - l_2)}{\{(x_1 - l_1)^2 + z_1^2)\}r_2} - \frac{(x_1 + l_1)(y_1 + l_2)}{\{(x_1 + l_1)^2 + z_1^2\}r_4}\right]\right\}$$

$$G_l^B(0/r_1) = B_z(x_1,y_1,z_1) = \mu_0(H_z^x + H_z^y) \tag{A.1}$$

where

$$r_1^2 = (x_1 - l_1)^2 + (y_1 - l_2)^2 + z_1^2$$

$$r_2^2 = (x_1 + l_1)^2 + (y_1 - l_2)^2 + z_1^2$$

$$r_3^2 = (x_1 - l_1)^2 + (y_1 + l_2)^2 + z_1^2$$

$$r_4^2 = (x_1 + l_1)^2 + (y_1 + l_2)^2 + z_1^2.$$

The vector potential $\bar{A}$ now has two components: A_x and A_y. These are given by

$$A_x = \frac{\mu_0}{4\pi}\left[\log\frac{(x_1 - l_1) + r_1}{(x_1 - l_1) + r_3} - \log\frac{(x_1 + l_1) + r_2}{(x_1 + l_1) + r_4}\right]$$

$$A_y = \frac{\mu_0}{4\pi}\left[\log\frac{(y_1 - l_2) + r_2}{(y_1 - l_2) + r_1} - \log\frac{(y_1 + l_2) + r_4}{(y_1 + l_2) + r_3}\right].$$

Thus

$$\bar{A} = (\bar{a}_x A_x + \bar{a}_y A_y) \tag{A.2}$$

where $\bar{a}_x, \bar{a}_y$ are unit x- and y-directed vectors.

If the vector potential $\bar{A}$ due to the loop side is to be calculated on itself, it is necessary to assume the current on that side is uniform over a strip $2l_2$ wide (see Fig. 5). Then the product $\int \bar{A}\cdot\bar{I}\,dl$ is estimated ($I = 1$):

$$\int_{\text{self}} \bar{A}\cdot\bar{I}\,dl = \frac{2}{l_2}\left[l_1 \log\frac{l_2 + (l_1^2 + l_2^2)^{1/2}}{l_1} + l_2 \log\frac{l_1 + (l_1^2 + l_2^2)^{1/2}}{l_2}\right]. \tag{A.3}$$

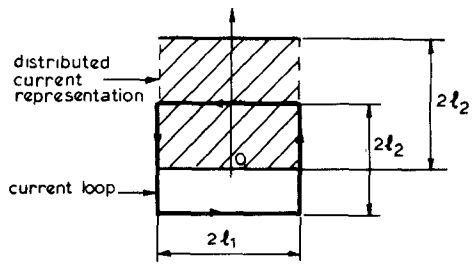

Fig. 5.

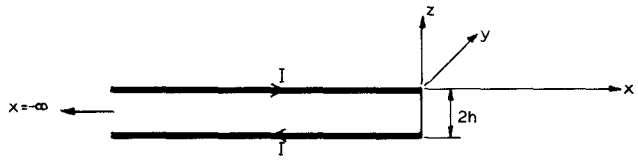

Fig. 6.

APPENDIX II
GREEN'S FUNCTIONS FOR SEMI-INFINITE LINE

In this case we assume the semi-infinite line is filamentary with unit current and the ground plane can be replaced by the image distance $2h$, with the return unit current (Fig. 6). It can be shown that

$$G_s^B(0/r_1) = B_z \text{ at } P(x_1,y_1,z_1)$$

$$= \frac{\mu_0}{4\pi}\left[\frac{y_1}{[x_1 + (x_1^2 + r_1^2)^{1/2}](x_1^2 + r_1^2)^{1/2}}\right.$$

$$\left. - \frac{y_1}{[x_1 + (x_1^2 + r_2^2)^{1/2}](x_1^2 + r_2^2)^{1/2}}\right] \tag{A.4}$$

where

$$r_1^2 = y_1^2 + z_1^2$$

$$r_2^2 = y_1^2 + (z_1 + 2h)^2.$$

It can also be shown that the vector potential $\bar{A}$ at P is given by

$$A_x(x_1,y_1,z_1) = \frac{\mu_0}{4\pi}\log\frac{x_1 + (x_1^2 + r_2^2)^{1/2}}{x_1 + (x_1^2 + r_1^2)^{1/2}}. \tag{A.5}$$

REFERENCES

[1] A. Farrar and A. T. Adams, "Computation of lumped microstrip capacitances by matrix methods—Rectangular sections and end effects," *IEEE Trans. Microwave Theory Tech.* (Corresp.), vol. MTT-19, pp. 495–496, May 1971.

[2] ——, "Matrix method for microstrip three-dimensional problems," *IEEE Trans. Microwave Theory Tech.*, vol. MTT-20, pp. 497–504, Aug. 1972.

[3] D. S. James and S. H. Tse, "Microstrip end effects," *Electron. Lett.*, vol. 8, pp. 46–47, 1972.

[4] I. Wolff, "Statischie Kapazitaten von Rechteckigen und Kreisformigen Mikrostrip—Scheibenkondensatorem," *Arch. Elek. Ubertragunstechn*, vol. 27, pp. 44–47, 1973.

[5] R. Horton, "The electrical characterization of a right-angled bend in microstrip line," *IEEE Trans. Microwave Theory Tech.* (Short Papers), vol. MTT-21, pp. 427–429, June 1973.

[6] ——, "Equivalent representation of an abrupt impedance step in microstrip line," *IEEE Trans. Microwave Theory Tech.* (Short Papers), vol. MTT-21, pp. 562–564, Aug. 1973.

[7] a) B. Easter, J. G. Richings, and I. M. Stephenson, "Resonant techniques for the accurate measurement of microstrip properties and equivalent circuits," in *Proc. 1973 European Microwave Conf.* (Brussels, Belgium), 1973, Paper B7.5.
b) B. Easter, private communication, 1973.

[8] A. Gopinath and P. Silvester, "Calculation of inductance of finite-length strips and its variations with frequency," *IEEE Trans. Microwave Theory Tech.*, vol. MTT-21, pp. 380–386, June 1973.

[9] A. F. Thomson and A. Gopinath, "Calculation of microstrip discontinuity inductances," to be published.

[10] a) P. Benedek and P. Silvester, "Equivalent capacitances for microstrip gaps and steps," *IEEE Trans. Microwave Theory Tech.*, vol. MTT-20, pp. 729–733, Nov. 1972.
b) ——, "Microstrip discontinuity capacitances for right-angle bends, T junctions, and crossings," *IEEE Trans. Microwave Theory Tech.*, vol. MTT-21, pp. 341–346, May 1973.

[11] A. Gopinath, R. Horton, and B. Easter, "Microstrip loss calculations," *Electron. Lett.*, vol. 6, no. 2, pp. 40–41, 1970.

[12] P. Silvester, "TEM properties of microstrip transmission lines," *Proc. Inst. Elec. Eng.*, vol. 115, pp. 43–48, Jan. 1968.